21. VALIDATION OF PHOTOMETRIC RESULTS

The Hipparcos photometric solution was one of the highlights of the mission and proved to be very successful. As was done for other parameters determined from the Hipparcos observations, the aim of this chapter is to provide an evaluation of the quality of the results from the study of the internal consistency and, when this was possible, from direct comparisons with ground-based data of comparable quality. Various aspects are taken up successively: the reliability and the precision of the calibration and in particular the error of the zero-point, the meaning of the internal errors published in the Catalogue with their relation to the true errors, the stability of the photometric system over the three years of instrument ageing and the validity of the period determination of newly identified periodic variables. Comparisons with three ground-based photometric systems show both the overall reliability of the data, as well as some of the features encountered when combining Hipparcos and ground-based photometry.

21.1. Introduction

Chapter 14 of this Volume presents the methods and algorithms that were developed and implemented to compute the magnitudes of all the Hipparcos programme stars. The magnitude estimates were obtained at every field transit, providing an average of 110 observations per star. This proved to be a rather complex task: starting from the recorded photon counts as indicators of the stellar intensity and relying on a set of photometric standard stars, defined within the assumed photometric system, instrument parameters were derived that determined the transformation of the observed intensities to magnitudes in this photometric system. At various stages of the processing the photometric system and the associated values of the photometric standard stars were re-adjusted and followed by a complete re-reduction of all photometric data available at that time (see also Section 14.5). An internal assessment of the quality of the final product was highly desirable and could be based on the consistency of all the determinations, the demonstration of the stability of the calibration from the fluctuation of the individuals measurements of known (or assumed) constant stars. From this analysis and the knowledge of the various noise contributions considered, our expectation was that the internal accuracy at the grid-crossing level was about 0.012 mag for a single measurement of a star of $Hp = 8$ mag.

Comparisons with ground-based systems may tell us more about the ground-based system than about Hipparcos, but a good agreement between well calibrated independent systems does provide a clear indication of the level of reliability of the Hipparcos photometry.

21.2. Evaluation of the Calibrations

As explained in Chapter 14, both FAST and NDAC used an instrument model to represent the sensitivity of the Hipparcos detection chain as a function of the position of the stellar image on the grid and of the colour of the star. The basic term of this calibration is the zero-point coefficient, representing the response of the detector at the centre of the grid for a star of colour $V - I = 0.65$ mag. Its variation with time mirrors the slow decline of the overall photometric response of the instrument, due mainly to the transmission loss in the glass of the optical elements of the main detection chain. This process was referred to as ageing. While the absolute value of the zero-point is rather arbitrary and has no deep physical meaning, the scatter of the zero-point about the mean ageing curve and the way the zero-points of the preceding and following field behave are very relevant to assess the ultimate accuracy of the calibration and as a consequence, that of the photometric solution.

Figure 21.1 shows the variations of the zero-point over the mission, expressed in magnitude. The origin of the scale was chosen to be close to the theoretical mid-mission, where the Hipparcos photometric scale was defined through the predicted magnitudes of the set of photometric standards. The plot gives the history of the zero-point for the dc-scale with the preceding field of view on the left scale and the following field of view on the right. The points on these curves are computed as $-2.5 \log X_1$ where X_1 is the FAST zero-point defined in Table 14.5. The ageing has been analysed in Chapter 14 and will not be reconsidered here. What is more important in the context of the validation of the photometric solution, is the fact that the same details appear in the two curves at the same time, although the calibrations for the two fields of view were fully independent and used different observations obtained within the same orbit. Several small incidents are visible on both curves and should be considered significant. See for example the small loss of sensitivity of about 0.02 mag at day $\simeq 600$, or the isolated increase of the same amplitude at day 934. The complex fine structures around days $\simeq 700$ are very similar in the two field of views. The same details can be observed from the equivalent NDAC calibration values (see Figure 14.4). The occurrence of these synchronous changes with the same amplitude makes us confident that these effects were real and not artifacts, and that they were properly accounted for by the calibrations that were performed twice a day during the mission.

Figure 21.2 shows the evolution of the difference between the zero-points of the preceding and following field of view. The observed difference is close to zero. This is not a chance effect, as most of the optical and detector chain is identical for the two fields of view. The precise value of the difference is, however, of little or no meaning. On the other hand the fluctuations of the distribution are much more relevant. The long term fluctuations are real and indicate small sensitivity variations that were not perfectly identical in the two fields of view. Similar variations between the two fields of view have been observed for a wide range of parameters (see, for example, Chapters 8 and 10). The overall variation of sensitivity has been of order 0.5 mag over the mission (Figure 21.1). However the evolution of the difference between the two fields, up to the

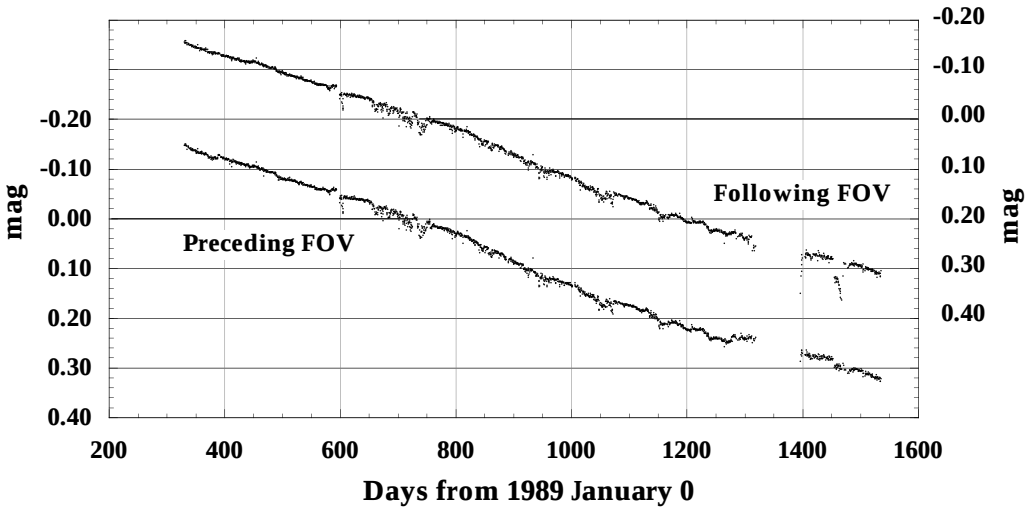

Figure 21.1. *Time variation of the zero-point of the photometric calibration for the dc-magnitude scale. The left scale refers to the preceding field of view (FOV) and the right scale to the following. The two scales in the plot have been shifted by 0.2 mag for better visibility; however the absolute value of the two sensitivities are very similar and should be very close at about day 700.*

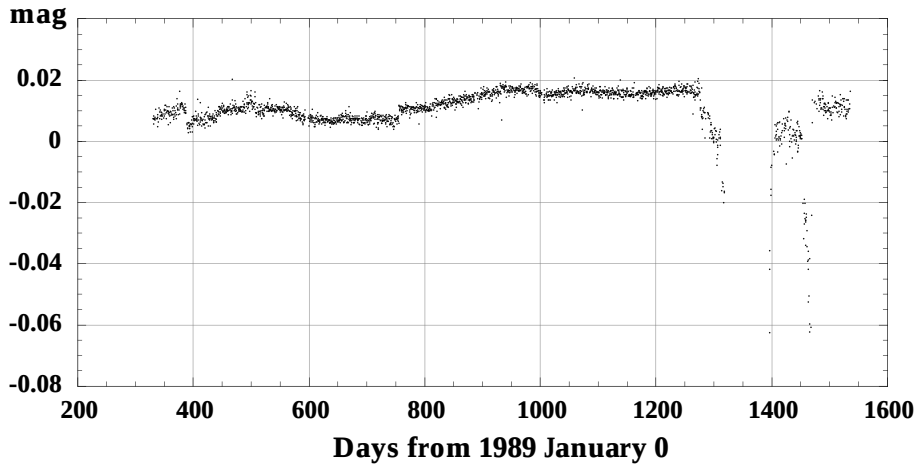

Figure 21.2. *Zero-point differences between the photometric calibrations of the preceding and following fields of view during the mission. The plot refers to the dc-photometric scale.*

start of the gyro problems at day 1250, remained within ±0.01 mag and was perfectly monitored by the calibration. During the sun-pointing mode and at the end of the mission the two fields started behaving differently. This could be contributed to changes in the temperature of the spacecraft, and the effects thereof on the optical system.

Also noted were a few discontinuities revealing quick changes in the instrument or in the calibrations as at day 388, with an increase of 0.003 mag in the sensitivity of the preceding field or the event of day 755 of 0.006 mag in the other direction and which in fact was not transient. The first event was caused by the implementation of the calibrated grid rotation in the observations, causing a general improvement in the pointing of the instantaneous field of view. The latter event was associated with a failure

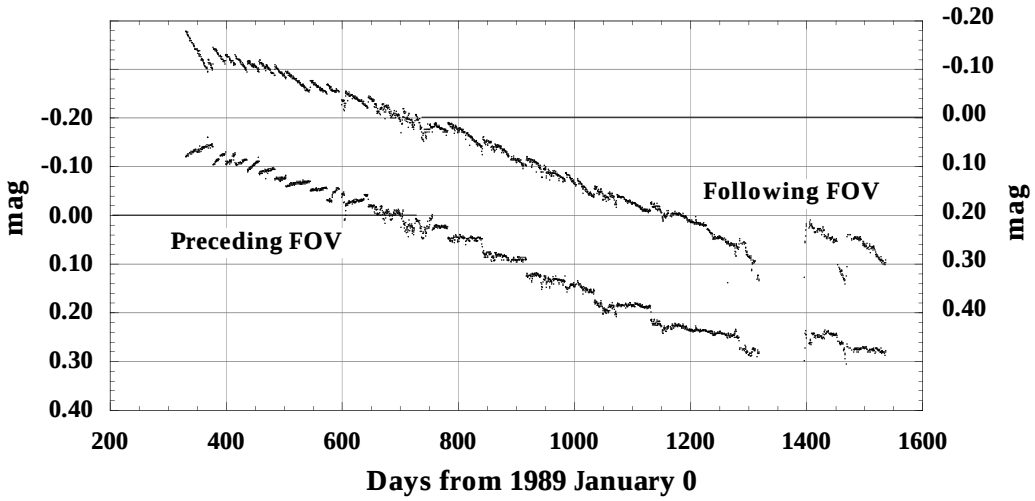

Figure 21.3. *Time variation of the zero-point of the photometric calibration for the ac-magnitude scale. The left scale refers to the preceding field of view (FOV) and the right scale to the following field of view. The two scales have been shifted by 0.2 mag for better visibility; however the absolute value of the two sensitivities are very similar.*

of the Thermal Control Electronics (TCE1), and a switch to the redundant system (TCE2) (see Table 2.1). These small changes in sensitivity were all properly restored by the photometric calibration which guaranteed the consistence of the photometric system to within a few millimagnitudes.

On a shorter time scale, the width of the curve is of the order of 0.003 mag and variations are of a random nature. This provides information on the amplitude of the statistical fluctuations of the calibration from one orbit to the next. It provides an indication for the ultimate quality of a calibration, which is about 0.002 mag in each field of view. This means that the individual Hipparcos photometric measurements are not defined in an absolute sense with an accuracy better than 0.002 mag. The internal consistency of the photometric system is, however, much better defined. For a constant bright star, the accuracy and stability of the instrument modelling, the zero-points and the chromatic parameters, were the limiting factors in the error budget of the accumulated photometry. For fainter stars, the photon statistics was the primary contributor to the errors.

A similar investigation was performed for the ac-scale, and led to the plots shown in Figure 21.3 for the evolution of the photometric response at the centre of the field for a star of colour index $V - I = 0.65$ mag and in Figure 21.4 for the difference between the two fields of view. The overall ageing is the same as for the dc-scale with a total decrease of the sensitivity of about 0.45 mag over the mission. The curves are however more structured over short timescale than for the dc-scale.

This becomes more clear by looking at the differences between the two fields of view in Figure 21.4. The long filaments going downward extending over one month at the beginning of the mission and two months later on, are associated to the slow change of focus, followed by the abrupt refocusing of the instrument (see also Figure 14.3 and Chapter 2 of this Volume, and Chapter 10 of Volume 2). As explained in Chapter 14, the ac-photometric scale is based on the amplitude of the modulation IM_1, where M_1 is the modulation coefficient of the first harmonic. (The exact formula is slightly

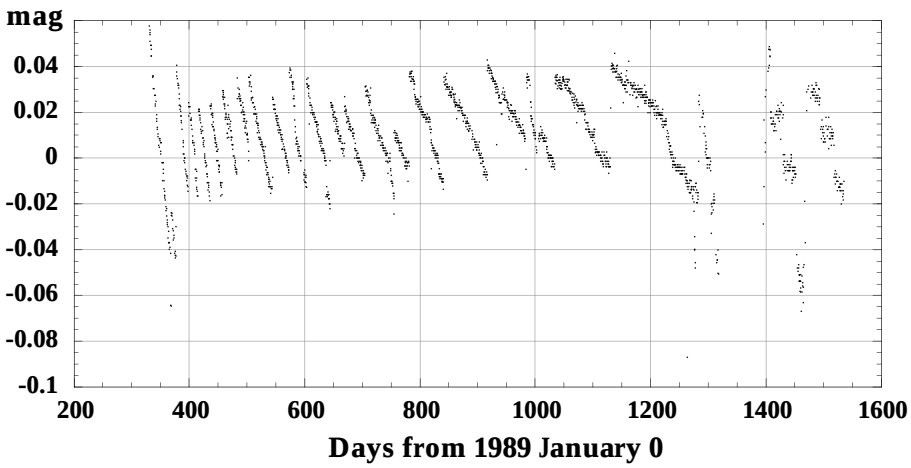

Figure 21.4. *Difference between the zero-points of the photometric calibration of the preceding and following fields of view during the mission. The plot refers to the ac-photometric scale. The thread-like features are due to slow changes in focus, the discontinuities are the result of refocusing.*

different for FAST, but this is of no importance here.) The zero-point of the ac-scale was therefore directly affected by the change in the modulation coefficient M_1, and thus by the refocusing, which produces a change in modulation and thus in the apparent sensitivity. The refocusing is global and does not have the same effect in the preceding and following field of view. From Figure 21.3 it is evident that the average sensitivity of the preceding field of view, as far as it can be measured by the zero-point, gets larger just after a refocusing took place whereas it decreases in the following field. This differential behaviour shows up amplified in Figure 21.4 as a significant difference in the zero-points according to the field of view.

21.3. Distribution of the Unit-Weight Variance

The Overall Distribution

The aim of this section is to investigate the reported standard errors of the photometric transits in order to assess whether they are representative of the true errors. The best way would be to study the true error of the Hipparcos photometry with respect to ground-based photometric measurements of comparable or better quality, and more or less obtained at the same time. Unfortunately few such measurements are available, and when they are, there remains the problem of transforming from the ground-based photometric system to Hipparcos, or *vice versa*, with an accuracy of few millimagnitudes.

The approach adopted here instead was to study the statistical distribution of the errors. Basically the scatter about the mean or the median of the 40 to 380 individual magnitudes of a constant star, should be related to the standard error given for the individual transits. If the standard errors are too optimistic the scatter appears too large and one can conclude that there is a lack of consistency. This is equivalent to studying the χ^2 distribution of the deviation of the individual measurements with respect to the median.

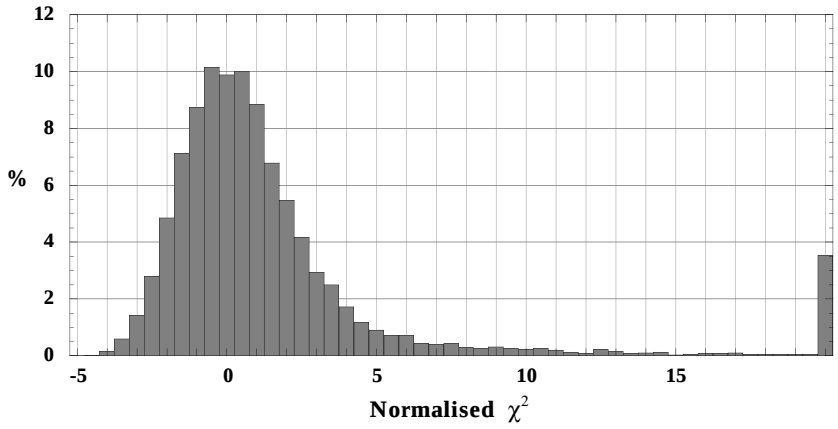

Figure 21.5. *Distribution of the reduced unit-weight variance of Hp in the Wilson-Hilfert normal approximation.*

For the ith star and the magnitudes Hp_{ij} obtained at the times t_j with the standard deviations σ_{ij} and a median of Hp_i, one has:

$$\chi_i^2 = \sum_{j=1}^{n_i} \frac{(Hp_{ij} - Hp_i)^2}{\sigma_{ij}^2} \qquad [21.1]$$

which follows a χ^2 distribution with $\nu_i = n_i - 1$ degrees of freedom. The Wilson-Hilfert cube root transformation has been used (Kendall & Stuart 1977) in the analysis because it gives a remarkably useful normal approximation to the χ^2 distribution as:

$$\mathcal{Z} = \left(\frac{9\nu}{2}\right)^{1/2} \left[\left(\frac{\chi^2}{\nu}\right)^{1/3} + \frac{2}{9\nu} - 1\right] \qquad [21.2]$$

which follows asymptotically a normal law with zero mean and unit variance.

For constant stars with Gaussian errors, the distribution of the $\mathcal{Z}(\chi_i^2)$ should be close to a standardized normal. When the star is variable, the systematic deviations from the mean are larger than the deviation expected from the purely random noise, since the total variance of the time series is the combination of the random component and that brought about by the true light variations. As explained in Volume 1, Section 1.3, Appendix 2, the χ^2 has been one of the basic variability indicators. Thus it is not possible to eliminate the variable stars to determine whether the χ^2 distribution of the remaining stars is adequately distributed. It should be the case by construction.

What has been done is the following: the negative range of $\mathcal{Z}$ predominantly comprises constant stars, even though just about the same number are in the positive region, but indistinguishable from the population of the true variables which are there as well. The argument is supported by the distribution of the reduced χ^2 in its Wilson-Hilfert version, shown in Figure 21.5. Roughly, from $-5 < \mathcal{Z} < 5$ there is a somewhat symmetrical distribution centred around $\mathcal{Z} = 0$, as expected.

The fact that the maximum of the distribution is about $\mathcal{Z} = 0$, is equivalent to saying that the unit-weight variance of the constant stars does not depart from unity on average. As a consequence for the bulk of the catalogue the standard errors of the accepted photometric transits are representative of the scatter observed between the individual transits and may be considered as realistic. Later in this section the particular case of the bright end will be considered separately.

Focussing on the positive range of the distribution, the population of the classes with $\mathcal{Z} > 2$ are systematically larger than their negative counterpart, indicating the presence of variable stars of small amplitude or with short duty cycle like the eclipsing binaries. The extension of the distribution to larger $\mathcal{Z}$ values is entirely populated by variable stars. Altogether there are 41 per cent of the stars with $\mathcal{Z} < 0$, 48 per cent with $0 < \mathcal{Z} < 5$ and 11 per cent with $\mathcal{Z} > 5$. So there must be from this distribution 7 per cent of weak variables and 11 per cent of perfectly detectable variables, i.e. about 13 000 such cases. This is the population of stars flagged U, M or P in Field H52 of the Hipparcos Catalogue.

Consider now the χ^2 distribution of the 41 per cent of the stars which show less scatter about the mean than expected. This amounts approximately to the 46 000 entries with the flag C in Field H52; the tests applied were not strictly the χ^2. Ideally, for a homogeneous population, the negative region of Figure 21.5, should be similar to the negative region of a standard normal law of zero mean and unit standard deviation. To see that better, a plot of the distribution and its mirror image with respect to $\mathcal{Z} = 0$ has been drawn (Figure 21.6).

By construction it is perfectly centred and symmetric, but its width is related to the scatter of the χ^2 of the constant stars. The standard deviation of this distribution is very close to 1.5 and a normal distribution of zero mean and $\sigma = 1.5$ is also plotted (the solid line in Figure 21.6). Other estimates of the standard deviation of the distribution can be obtained by restricting to the distribution shown in Figure 21.5 by using the quantiles < 0.5. With the quantiles 0.2, 0.3, 0.4 one gets for the standard deviation of the assumed normal distribution 1.53, 1.52 and 1.5 respectively. The mean of the distribution for $\mathcal{Z} < 0$ is under the normal assumption $\sigma\sqrt{2/\pi}$. The observed mean of $\mathcal{Z}$ with $\mathcal{Z} < 0$ is 1.19, which yields for the estimate of $\sigma \simeq 1.49$. Finally the same study has been made by partitioning the stars according to their brightness using four classes of similar size with $Hp < 7.5$ mag, 7.5 mag < Hp < 8.5 mag, 8.5 mag < Hp < 9.5 mag and $Hp > 9.5$ mag which happen to be centred on Hp = 7, 8, 9 and 10 mag. The respective standard deviations are 1.56, 1.60, 1.52, 1.48.

This phenomenon cannot be ascribed simply to a mere scale factor in the standard errors, since this would also change the mean dramatically and make the mode of the χ^2 distribution much larger than unity, even for a small underestimation of the standard error (and much smaller than unity for a small overestimation). It seems to indicate rather that the population is not a homogeneous one, even after scaling by the standard deviation, and there are some categories of stars where the standard deviation is too small compared to the actual scatter and other groups where just the opposite conclusion applies. On the average the distribution remains well centred, but its negative wing gets wider due to the population with too large standard errors which displaces the whole distribution to the left. A more detailed investigation of this effect goes beyond the objectives of this volume, but is worth doing in the future.

Bright Stars

For the bright stars an investigation has been conducted to determine the χ^2 distribution within each class of magnitude. In the Hipparcos Catalogue there are 1473 stars brighter than Hp = 5 mag consisting of 1264 single stars and 209 double and multiple stars. Obviously the recognition of the variability becomes much more sensitive for these stars and the χ^2 distributions show extended positive wings with significant population. The

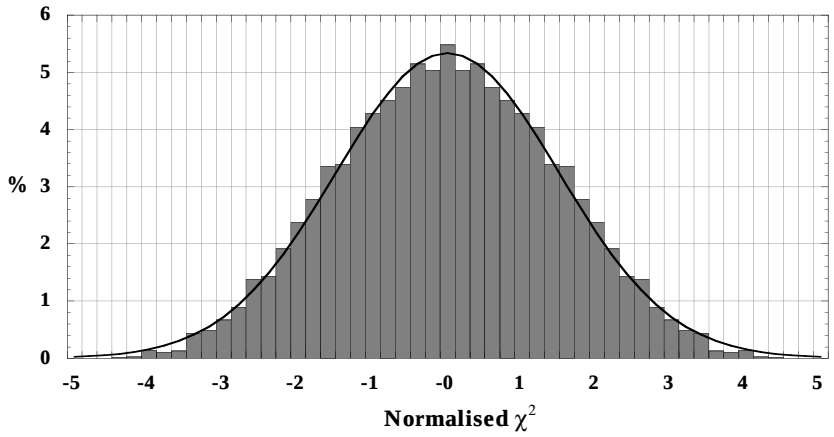

Figure 21.6. *Symmetrised distribution of the unit-weight variance of Hp.*

Table 21.1. The unit-weight variance for the bright stars as a function of *Hp*. The second line gives the average of the reduced χ^2 for the constant stars within a class of magnitude. The factor κ represents the coefficient by which the standard deviations should be multiplied to make the χ^2 centred at one.

Hp	1.0	1.5	2.0	2.5	3.0	3.5	4.0	4.5	5.0
χ^2	4	3.4	2.8	2.2	1.9	1.5	1.3	1.1	0.99
κ	2	1.85	1.67	1.48	1.38	1.25	1.14	1.04	1.00

number of stars in each class is too small to apply the symmetrised distribution used above to a sub-population assumed to comprise only constant stars.

Instead, stars with $Hp_{\min} - Hp_{\max} < 0.02$ mag have been considered as constant and the median of their χ^2 distribution has been computed as a function of the magnitude. It departs markedly from one as shown in Table 21.1. Interpreting this offset as an underestimation of the standard errors, one can determine the factor κ by which one should multiply the standard errors to scale down the unit weight variance.

21.4. Analysis of the Periods of Variable Stars

Period searches were undertaken for stars detected as variable from the variance analysis. Several methods were applied to determine reliable periods, usually using a Fourier analysis as a first step. However severe limitations were placed on the efficiency of any method as a result of the poor and irregular time coverage of the observations. The character of the scanning law made the period recognition particularly difficult in the range 5 to 100 days. A description of some of the methods actually employed is given in Section 1.3 of Volume 1.

For many variable stars, a ground-based determination of the period is available and can be used to assess the quality of the Hipparcos determination based only on the observations made during the mission. There are a total of 2541 periods that were successfully computed from the Hipparcos data, of which 1272 have a ground-based

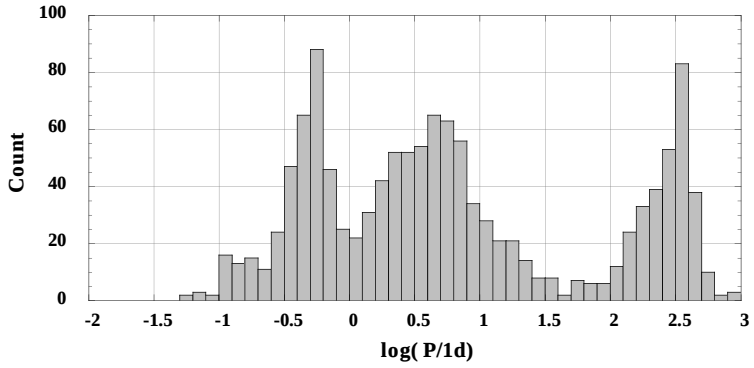

Figure 21.7. *Distribution of the periods of periodic variable stars computed from the Hipparcos data for which a ground-based determination is known. The abscissa gives the logarithm of the period expressed in days.*

counterpart and 1269 can be considered as new determinations, as far as the search in the literature can be considered as comprehensive, a goal almost impossible to fulfill. These figures should be regarded as a good order of magnitude for each category.

The period distributions for the two groups are shown in Figure 21.7 and Figure 21.8. The two distributions are broadly similar but differ in the details. They cover the same range of periods from about one hour to 1000 days. The upper limit is smaller for Hipparcos newly determined periods, with an upper bound of about 500 days, i.e. half the mission duration. The ground-based periods covers roughly three regions centred at 5 hours, 4 days and 250 days with a significant depletion at $P \simeq 40$ days. As for the distribution of the new determinations many periods appear in the range 0.6 days to 5 days, with a regular decrease in the detection of larger periods. The decrease in number of periods just above 5 days should be ascribed to the observation window which makes the period analysis difficult in this range. The depletion at about 40 days is less prominent than in the case of the periods with ground-based measurements, but this could also be due to the window function: periods in that range could quite easily have been wrongly assigned.

To judge the validity of the period determination relying only on the Hipparcos data, it is useful to compare the 1272 determinations which have an equivalent from the ground, where it should be realized that there is considerable variation in the reliability of ground-based periods, as well as that some variable star periods are changing with time. A plot showing the ground-based period against the Hipparcos value is shown in Figure 21.9. It is found that $|\Delta P|/P$ is less than 1 per cent for 917 stars out of the 1272 examined, less than 10 per cent for 1150 and larger for the remaining $\simeq 100$. As a consequence most of the data points in Figure 21.9 lie along the first diagonal. The small straight spikes at periods 0.1, 0.2 and 0.3 days result from the rounding of periods in the published data.

In a logarithmic plot, all the data points well outside the first diagonal correspond to very large disagreement between the Hipparcos and the ground-based period. However as a rule, there is either a close agreement or a strong disagreement between Hipparcos and the ground-based data. As the period range of the new variable stars measured by Hipparcos is not very different from the periods measured in the set of known variable stars, we may infer that the new periods have the same level of reliability.

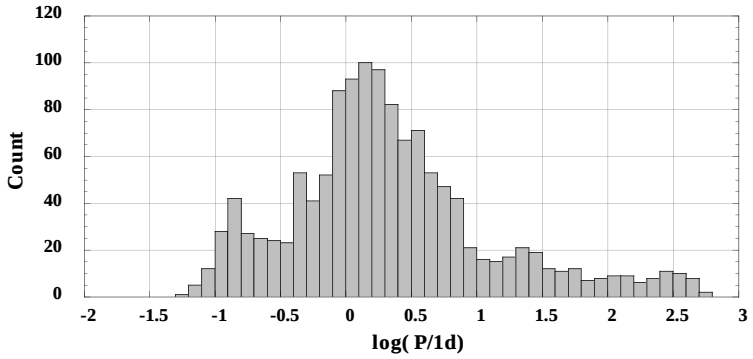

Figure 21.8. *Distribution of the periods of periodic variable stars computed from the Hipparcos data with no known ground-based determination. The abscissa gives the logarithm of the period expressed in days.*

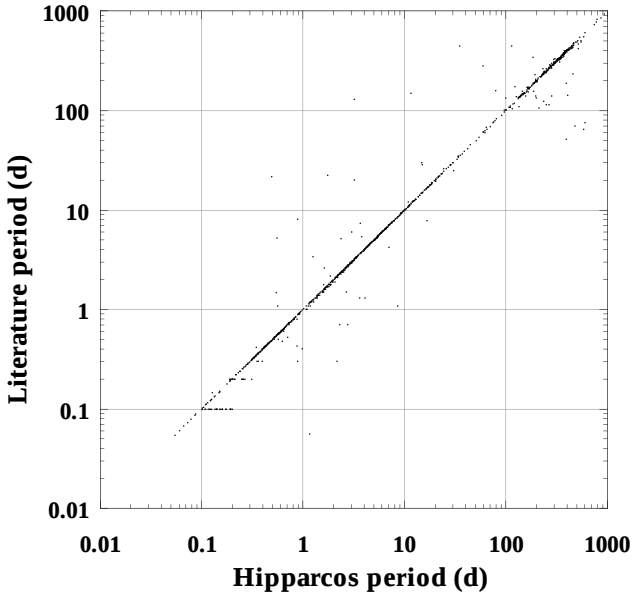

Figure 21.9. *Comparison of the periods of variable stars found in the literature to the determinations based only on the Hipparcos observations.*

21.5. Stability of the Photometric System

Selection of Constant Stars

The ageing of the instrument was significant during the mission, reaching 0.5 mag for a star with $V - I = 0.65$ mag as it was shown in Section 21.2. The effect was colour dependent, being more pronounced for the early type stars than for the reddest (see Chapter 14, Figure 14.4). Over the 37 months of observation, the calibration process intended to reduce all the observations onto a unique and constant photometric system, close to the actual sensitivity curve of Hipparcos at mid-mission. One way to check

Table 21.2. List and basic data on the ten constant stars that have been used in this work to determine the stability of the Hipparcos photometric system. N_1 = number of photometric transits, N_2 = number of accepted transits, Var. = Variability flag of the Hipparcos Catalogue.

HIP	HD	Sp.	$V-I$ mag	N_1	N_2	Var.	Hp mag	σ_{Hp} mag	$\sigma_{\rm transit}$ mag
11698	15596	G5 III	0.970	57	55	C	6.3760	0.0011	0.0062
13473	18149	F5 V	0.505	150	148	X	6.0318	0.0006	0.0064
34622	54810	K0 III	1.026	88	86	X	5.0792	0.0007	0.0049
37447	61935	K0 III	1.007	153	145	C	4.0986	0.0004	0.0039
41307	71155	A0 V	−0.024	75	71	C	3.8987	0.0003	0.0033
49712	88206	B3 IV	−0.100	149	126	X	4.8151	0.0006	0.0047
58345	103932	K4 V	1.219	92	86	X	7.0986	0.0009	0.0078
59750	106516	F5 V	0.526	143	133	X	6.2143	0.0007	0.0062
69722	124780	F0 V	0.335	82	82	X	6.6416	0.0007	0.0067
75181	136352	G2 V	0.715	80	76	C	5.7821	0.0007	0.0056

whether this goal was achieved is to investigate the 'light curve' of known constant stars. If the system remained well defined and constant during the mission, the scatter of the individual measurements about the mean should be compatible with the standard errors computed at the transit level and no trend should appear in the data between the beginning and the end of the mission (however, note that a trend could still appear if the wrong colour index had been applied for a star in its data reductions; see also Section 14.5).

The computation of the unit-weight variance has been the baseline to identify about 46 000 stars as constant, i.e. not detected as variable with the Hipparcos data. It would have been a vicious circle to select few constant stars from this sample to investigate the stability of the photometric system. Instead, a list of eleven photometric standards of various spectral types and classes has been kindly provided by E. Chapelier (private communication). One of the stars was detected and solved as double by Hipparcos and was not included in the analysis. The remaining ten stars should be photometrically constant at the level of 0.01 mag.

The list of selected stars is given in Table 21.2 with the spectra and colour of each star and the summary data of the Hipparcos observations. The number of accepted transits corresponds to the photometric transits considered as particularly reliable, with no anomaly detected. The median value of Hp and its standard error are based only on the accepted transits and are the same as the corresponding numbers given in the Catalogue. The last column gives the average of the standard errors of the individual transits for each star computed from the transit data in the Hipparcos Epoch Photometry Annex. The ratio between the numbers of the last two columns is always of the order of $\sqrt{N_2}$ as expected. The variability index is particularly interesting in the present context: only four of these stars were labelled constant and none was discovered as variable. Being 'constant' is an attribute which is not the opposite of being variable.

The individual observations are plotted in Figure 21.10 and Figure 21.11 as a function of the observation number. The data points appear in chronological order, but the scale is not linear with the time. However for every star there are observations performed during the first months and the last months of the mission. The error bars are given by the standard error of the individual transits published in the Hipparcos Epoch Photometric Annex. The full scale of the Y-axis is the same for all the plots with a range of 0.1 mag. From a visual inspection the distribution of the individual observations look very satisfactory at first glance. The stability of stars like HIP 41307 and HIP 75181 appears particularly outstanding.

Application of a χ^2 Test

For each star χ^2/ν and its $\mathcal{Z}$ approximation have been computed with Equations 21.1 and 21.2. Results shown in Table 21.2 indicate, as expected, no evidence of variability. However the values are large enough for HIP 37747 and HIP 49712 to exclude them from the category of constant stars, until further examination. For example, for HIP 37747, it appears that from the data points plotted in Figure 21.10, the large χ^2 value is based on a few measures that deviate from the median by several standard deviations and also because of a larger scatter at the end of the mission. A different test, able to locate outliers would probably conclude that this star is sufficiently stable to be classified as constant.

Study of the Range

The χ^2 is an all purpose test and is not always sensitive to all the possible defects of the photometric reduction. The columns $H_{\rm min}$ and $H_{\rm max}$ in Table 21.3 give respectively the magnitude for the observed maximum and minimum brightness, computed as the 5th and the 95th percentiles of the magnitudes measured at every field transit. The values have been recomputed from the transits data and have one more decimal figure than in the Catalogue. The range is the difference between these two numbers and under the assumption that the star is constant and the error Gaussian, the expectation of the range is 3.29 standard deviations. The observed and expected values are given in Table 21.3 as Δ_1 and Δ_2. They are relatively consistent with each other; the most significant departure being again HIP 37747 and to a lesser degree HIP 58345 and HIP 59750. For the other stars the agreement is very satisfactory.

With the results from the χ^2 tests, the following conclusions can be drawn:

(1) the estimate of the standard deviation at the level of the individual observations is compatible with the scatter of the observations, indicating that the errors given in the catalogue are probably realistic, except as noted earlier, for the very bright stars;

(2) for constant stars there is no large tail in the distribution of errors. Otherwise the test based on the range would have failed. This test is very sensitive to small departures from the expected distribution.

Testing for the Presence of Trends

The third study carried out on this set of constant stars aimed at detecting possible systematic trends with the time, a possibility arising as a result of the instrument chromatic ageing (see Section 14.5). A linear model $Hp(t) = \alpha + \beta(t - t_0)$ has been fitted to the data.

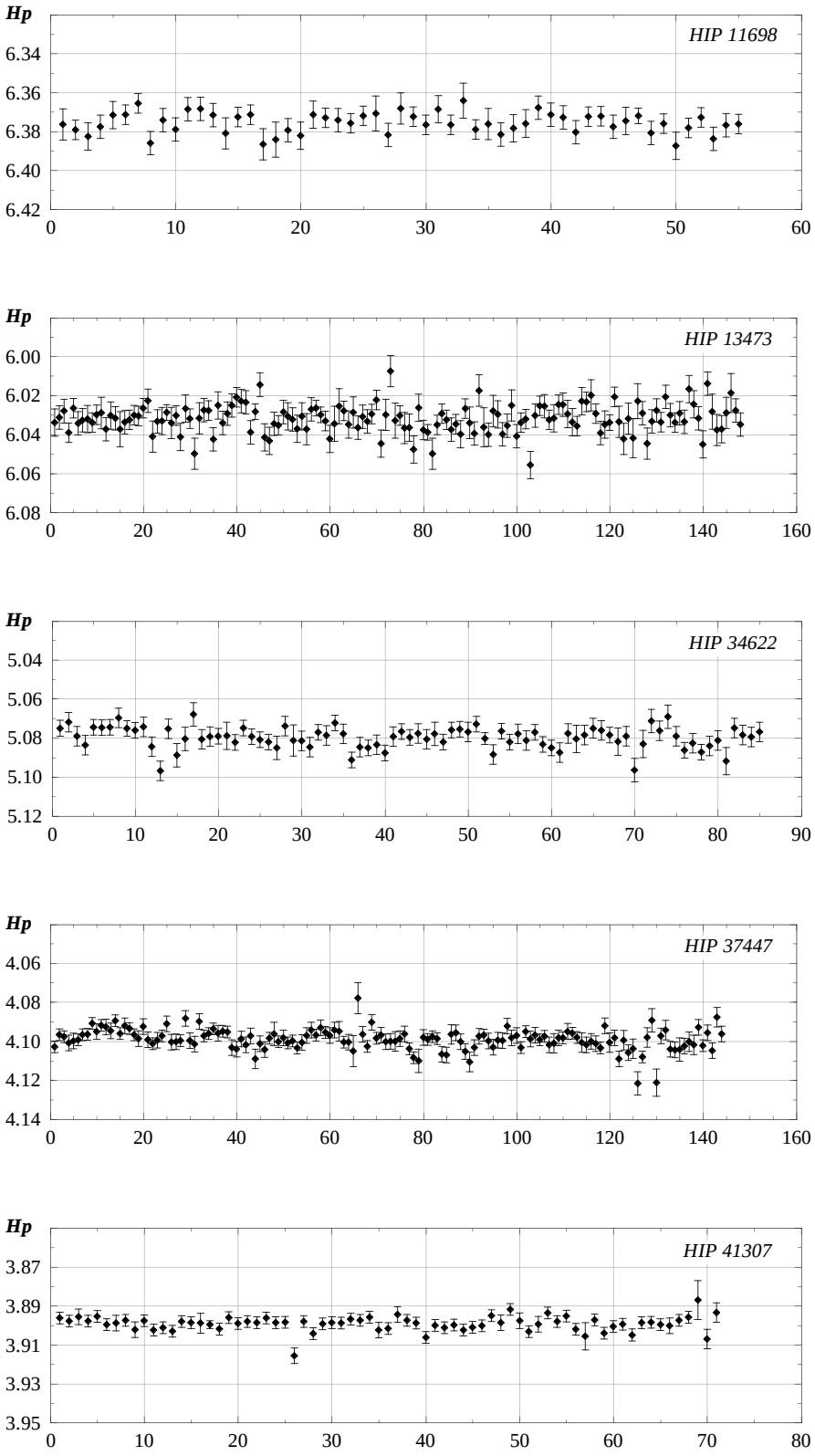

Figure 21.10. *Light curves based on the Hipparcos data for a sample of known constant stars. The observations are ordered according to the observation number in chronological order.*

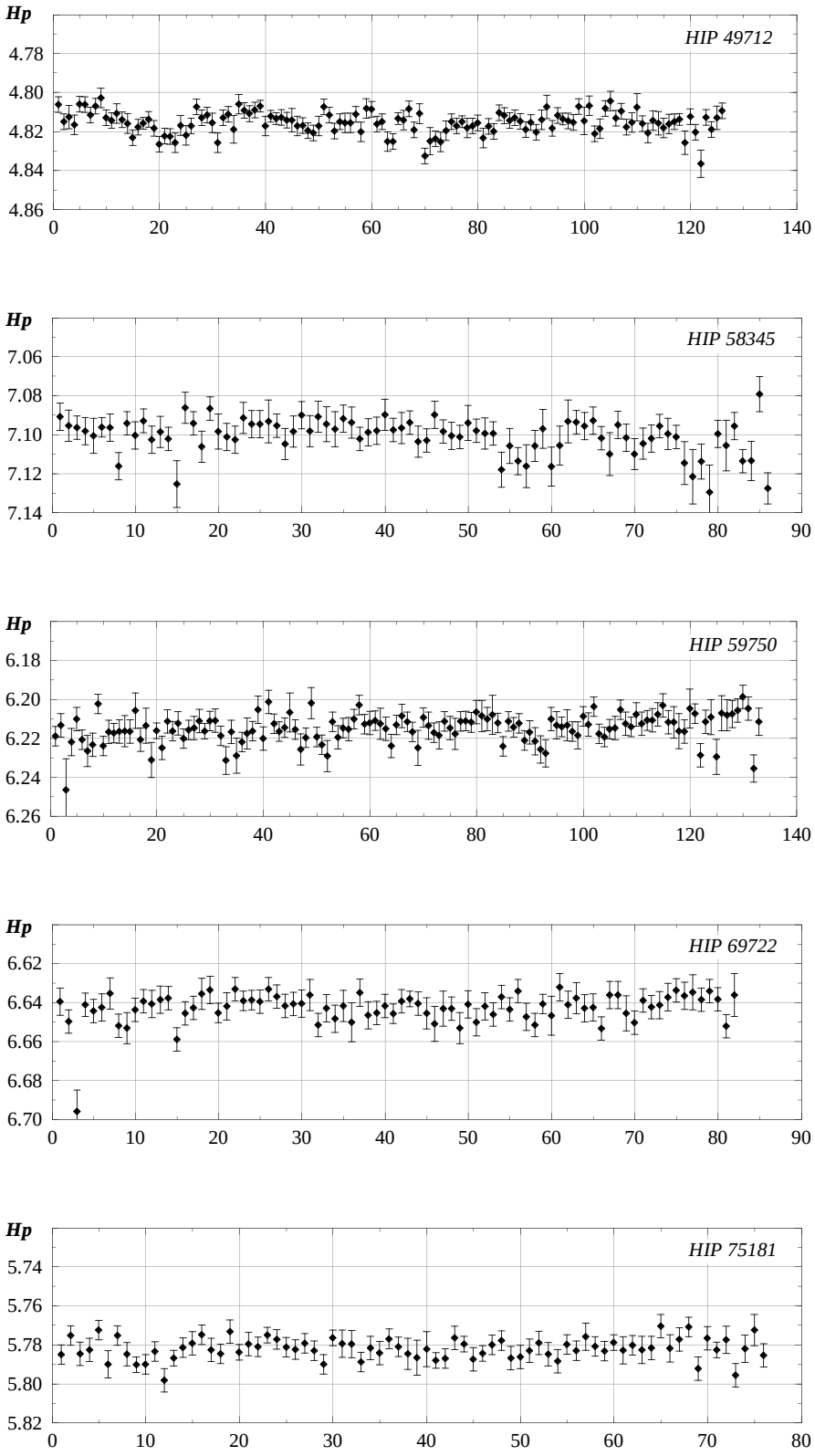

Figure 21.11. *Light curves based on the Hipparcos data for a sample of known constant stars. The observations are ordered according to the observation number in chronological order.*

Table 21.3. Summary results of the checks performed on the constant stars listed in Table 21.2. $\Delta_1 = H_{\min} - H_{\max}$, Δ_2 = its expected value with $\sigma_{\rm transit}$ of Table 21.2.

HIP	χ^2	$\mathcal{Z}$	$H_{\max}$	$H_{\min}$	Δ_1	Δ_2	Trend
			mag	mag	mag	mag	10^{-6} mag/day
11698	0.66	−1.95	6.367	6.386	0.019	0.020	+1.6 ± 2.6
13473	1.07	+0.59	6.020	6.044	0.024	0.021	−1.7 ± 2.0
34622	1.11	+0.70	5.071	5.091	0.019	0.017	+2.6 ± 1.9
37447	1.42	+3.16	4.090	4.108	0.018	0.013	+4.4 ± 1.4
41307	0.85	−0.89	3.894	3.906	0.012	0.011	−0.8 ± 1.7
49712	1.51	+3.49	4.806	4.826	0.019	0.016	+2.2 ± 1.6
58345	1.08	+0.55	7.090	7.120	0.031	0.026	+9.5 ± 2.9
59750	1.12	+0.99	6.204	6.229	0.025	0.020	−6.7 ± 2.1
69722	0.78	−1.44	6.634	6.653	0.020	0.022	−7.8 ± 3.8
75181	0.87	−0.78	5.772	5.791	0.018	0.018	−1.9 ± 2.2

The fitted gradient of the trend β is given together with its error in the last two columns of Table 21.3. The trend is just above the 3σ level for the same three stars for which the range was found anomalous. A trend between 4×10^{-6} to 9×10^{-6} mag per day is equivalent to a total systematic effect in the range 5 to 10 millimag over the mission. For the other stars the trend is totally negligible which confirms at the same time that these stars are not long period variables and that the Hipparcos photometric system does not change with the time. The fact that few stars exhibit a trend does not invalidate this conclusion: as was stated above, trends can be the result of errors in the colours used in the data reductions, and can occasionally be related to actual astrophysical phenomena. As long as the average star does not show a significant trend, it can be concluded that the photometric system is stable.

21.6. Comparison with the Walraven Photometric System

The Walraven photometric system (Lub & Pel 1977) is amongst the best internally calibrated systems. A complete recalibration of all available data has been undertaken by Lub & Pel, based upon a consistent programme of standard star measurements made between 1980 and 1985. This programme resulted in the complete redefinition of the *VBLUW* system of standard stars as it was available on the Dutch telescope at La Silla between 1979 and 1991. The system available prior to 1979 in South Africa, though closely related to the La Silla one, has to be treated separately and will not be further discussed here. Based upon the reductions which Lub provided for all available data, Pel produced a list of in total 1972 'calibration' stars of high quality observations, and

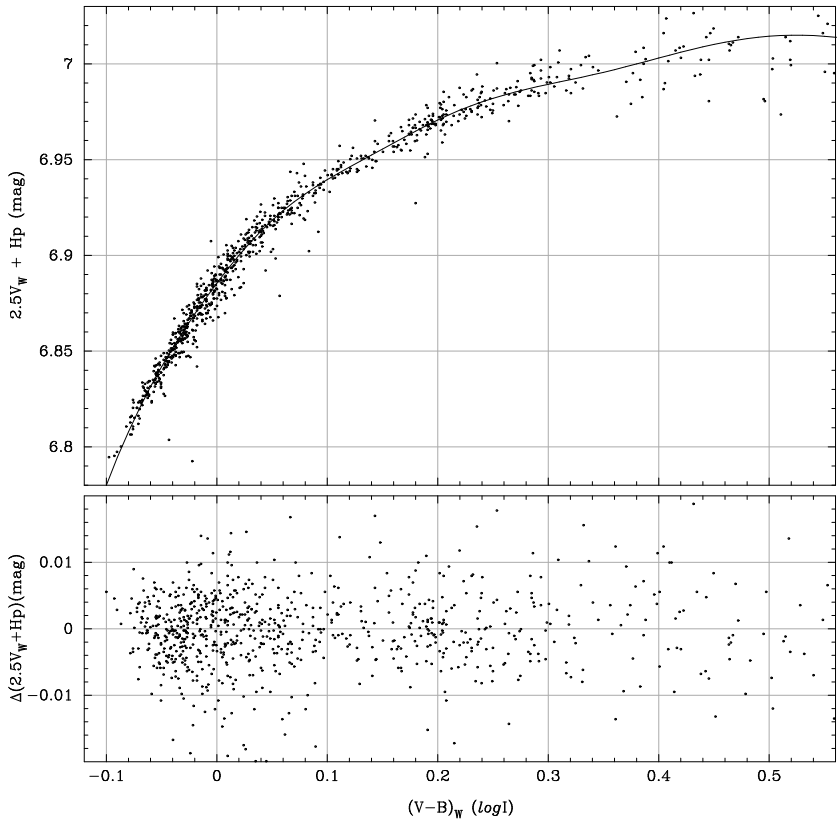

Figure 21.12. *Comparison of Walraven photometric V-band measurements with Hipparcos median Hp magnitudes. Above: the direct comparison of the data (the V_W is expressed in log I), and the fitted curve. Below: the residuals left after subtracting the fitted curve.*

spanning a large range of intrinsic properties, as a preparation to a full rediscussion of the merits of the *VBLUW* photometric system.

Pel (1991) applied this basic catalogue to an intercomparison between the four photometric systems with most data available in the southern hemisphere. Whereas the comparison with the Cousins' V magnitude and $(B-V)$ colour, and similarly with the Strömgren y and $(b-y)$ versus Walraven V and $V-B$ showed no clear systematic effects as a function of magnitude, colour, right ascension and declination, problems were encountered in the comparison with the Geneva V and $(B2-V1)$ (see also Section 21.7).

A comparison between two photometric systems will show that either one of the systems is having problems (without distinguishing which system), or that both systems are reliable at the level of detection. The chance of both systems being affected by exactly the same discrepancies is too small to be considered seriously, in particular when backgrounds of these systems are very different. Accordingly it was considered to be of great interest to compare the same high-quality catalogue with the Hipparcos photometry. Of the 1972 stars, 1720 were identified as Hipparcos stars (only the 1948 stars with HD numbers were checked), and of these 944 had a χ^2 based probability of being constant higher than 20 per cent.

In the comparison only 843 stars of luminosity classes III to V were used, after verification that there were no systematic effects observed between stars of these classes. Stars

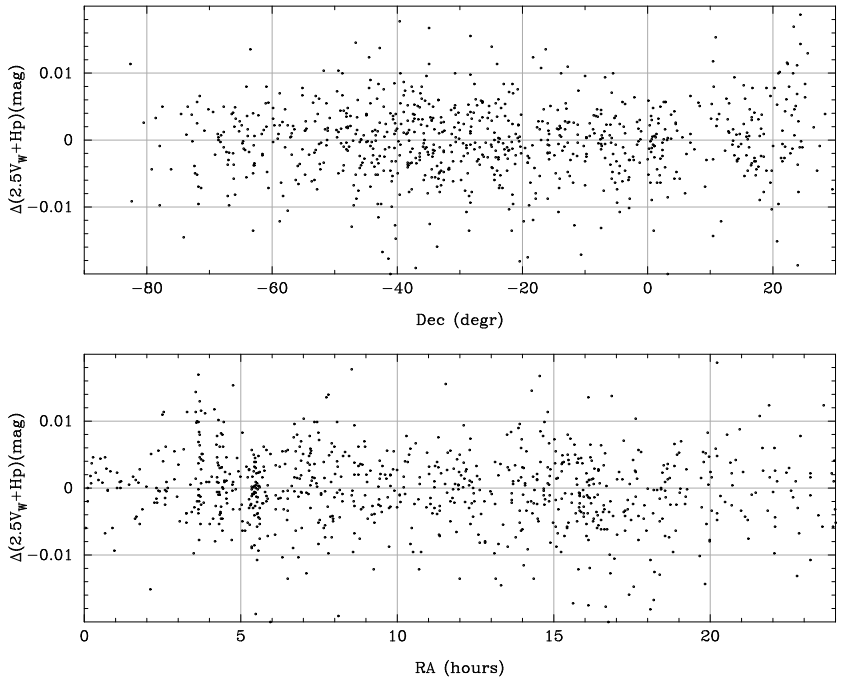

Figure 21.13. *The differences between Hp and transformed V_W magnitudes as a function of declination (top) and right ascension (bottom), showing no signs of dependence of residuals with position on the sky.*

detected as possibly variable had been excluded. Comparisons were made with respect to median Hp magnitudes in the Hipparcos system. In the Walraven system, all data are represented as $\log(I)$ values, which requires a multiplication by -2.5 to obtain the equivalent in magnitudes.

Figure 21.12 shows the comparison between the Walraven V and the Hp magnitudes, as a function of the Walraven $(V - B)$ index. As the system was originally intended for the study of early type stars, to which the sensitivity to a three-dimensional classification for the F and G stars was added later, the majority of comparison points are found among the B, A, F and G type stars. To every point an error was assigned, based on the error on the median as given in the Hipparcos catalogue, and the error on the mean for the Walraven data (the quoted standard deviation divided by the square root of the number of observations). The errors were dominated by the contribution from the Walraven system. The data were subsequently fitted with a cubic spline function, using 6 knots. The unit-weight standard deviation after this fit was 1.7, which may reflect the length of time covered by the Walraven data (> 10 years). There is also an indication that some of the remaining dispersion is still related to astrophysical properties: a comparison between the $(B - U)$ colour index and the remaining residuals showed some (difficult to represent) systematic behaviour. The remaining noise is at a level of 0.003 mag, which can be considered as very good for both the Hipparcos and the Walraven system. Systematic differences are well below the 0.001 mag level.

Figure 21.13 shows the residuals as a function of right ascension and declination. In some photometric systems there are small but significant calibration inconsistencies as a function of position on the sky, due to the complicated process of establishing a fully reliable calibration sequence in the presence of seasons and a fixed location. The

Table 21.4. Corrections needed to transform the V magnitudes in the main catalogue (Field H5) to Johnson V_J magnitudes for luminosity class III to V and spectral type O to G5.

$B-V$	Corr	$B-V$	Corr	$B-V$	Corr	$B-V$	Corr
−0.50	−0.0083	0.20	+0.0037	0.70	+0.0041	1.30	−0.0072
−0.40	−0.0068	0.30	−0.0007	0.80	+0.0032	1.35	−0.0086
−0.30	−0.0053	0.35	−0.0024	0.90	+0.0030	1.40	−0.0088
−0.20	−0.0034	0.40	−0.0018	1.00	+0.0020	1.50	−0.0070
−0.10	−0.0015	0.50	+0.0013	1.05	−0.0010	1.60	−0.0023
0.00	+0.0003	0.60	+0.0049	1.10	−0.0022	1.70	+0.0028
0.10	+0.0022	0.65	+0.0053	1.20	−0.0045	1.80	+0.0080

Walraven system appears to be free of systematic effects down to a level of at least 0.001 mag, and the same has to be true for the Hipparcos system (see also Pel 1991).

This comparison is, due to its limited range in colour, only providing information on the system quality for relatively blue stars ($B-V<1.3$), and it requires other systems to make similar comparisons for redder stars. However, the very good level of agreement shows that the Hipparcos system can be considered as internally consistent and very reliable for at least all but the most extreme-colour stars.

21.7. Additional Comparisons with Ground-Based Systems

The Magnitude Scale

The comparison of Hp magnitudes to ground-based data required a reduction of Hp to Johnson V_J magnitude through a single relation for stars earlier than G5 stars or with $(B-V)<0.9$, and relations distinct for giants and dwarfs of later type. The colour corrections are expressed as function of $(V-I)$ and lead to the V magnitude as given in Field H5 in the main catalogue (see Volume 1, Sections 1.3 and 2.1). The set of standard stars was obtained by reducing all data from the major photometric system to Johnson V, $(B-V)$ and Hp. The comparison of V, as provided in Field H5, with genuine UBV data shows small chromatic residuals (Table 21.4). They are to be added to the V given in the Hipparcos catalogue to obtain the Johnson V for O to G5 stars and later type red giants. Similar tables must be used to reproduce V magnitudes from different photometric systems.

Once corrected for chromatic residuals, V magnitudes from Hipparcos may be checked against ground-based data. The mean difference $V_J-V(Hp)$ is plotted as function of the visual V_J magnitude in Figure 21.14, retaining stars in common with Geneva photometry and UBV photometry respectively, and excluding M giants and variable stars. The common feature is a small but significant non-linearity with a mean slope of −0.0017 mag/mag in the range $V=3-9$ mag. The bump around $V=4.7$ mag is present both with UBV and Geneva data. This global behaviour is not understood and may be due to ground-based data as well as to Hipparcos instrumentation. The occurrence of similar departures for two distinct photometric systems is an indication that space magnitude scale may be slightly distorted. Uncertainty on the intensity transfer function would affect only the brightest stars.

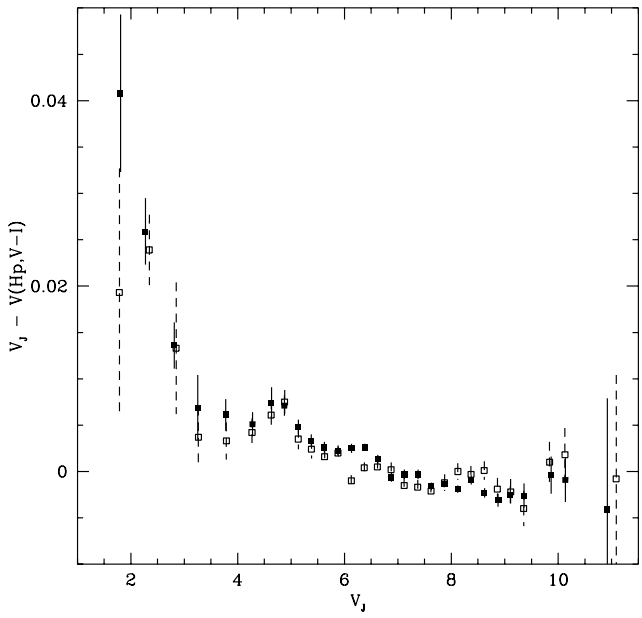

Figure 21.14. *The mean errors V(ground)-V(Hp) as a function of the apparent V magnitude from Geneva photometry (filled symbols) and from UBV photometry (open symbols).*

By construction the Hipparcos Hp system is tied to the UBV system by the relation: $Hp = V_J$ for $B - V = 0.000$ mag. With the above mentioned chromatic corrections the mean difference $\langle V_J(UBV) - V(Hp)\rangle$ is only −0.00006 mag for 15 386 non-variable comparison stars.

The Brightest Stars

The Hp magnitudes of the brightest stars show some departures from the expected magnitude computed from ground-based Johnson V_J or Geneva V(Gen), and colour correction $(Hp - V)$ derived from $(B - V)_J$ or $[B - V]_G$. The departure Hp(obs) − Hp(true) reaches 0.005 mag at $V = 3.5$ mag, and 0.025 mag at $V \simeq 2$ mag. A few stars around $V = 0$ mag show departures up to 0.04 mag. Hp magnitudes are slightly underestimated in the range 0 to 4 mag and overestimated if brighter than $V \simeq 0$ mag. This non-linearity effect is attributed to the satellite detection chain calibration and not to the ground-based photometry since the departures between observed and predicted Hp magnitudes are the same for two independent data sets, UBV and Geneva, obtained with different detectors.

The brightest stars are often used as spectro-photometric standards, like HIP 91262, α Lyr. The estimated Hp for the three brightest stars are given in Table 21.5 together with data from Geneva and UBV photometry. The other bright stars, with $V > 0$ mag, have observed Hp coherent with the prediction from ground-based photometry. For Sirius (HIP 32349), the photon flux from Hipparcos is underestimated by about 44 per cent. The reason for this discrepancy was the failure of the analogue mode for the image dissector tube (see Section 5.1), which forced the observations of Sirius to be made in

Table 21.5. Magnitudes for the brightest stars measured by Hipparcos, compared with measurements in the Geneva and the *UBV* systems.

Name	HIP	Hp	σ_{Hp}	Hp(Gen)	$Hp(UBV)$
Canopus	30438	−0.5536	0.0066	−0.678	−0.652
Sirius	32349	−1.0876	0.0024	−1.422	−1.453
Vega	91262	0.0868	0.0021	0.048	0.030

photon counting mode, even though it was evident that counts would be seriously affected by saturation.

The mean V magnitude for the primary standard Vega, HIP 91262, in *UBV* photometry is $V = 0.033 \pm 0.003$ mag with a range from 0.01 to 0.06 mag and few discrepant values up to 0.16 mag. Geneva $V = 0.028 \pm 0.004$ mag is consistent with the magnitudes as measured in the *UBV* and *WBVR* systems: 0.028 mag. A mean value $V_J = 0.030$ mag is adopted to tie the Hipparcos magnitude scale to the spectrophotometric data. With $B - V = -0.001$ mag, $Hp = 0.030 \pm 0.001$ mag for Vega. Table 21.5 provides a summary of the relevant photometric data for the brightest stars.

Photometric Precision

With the exception of a possible, small, systematic magnitude drift, the Hipparcos photometry shows the highest accuracy ever achieved in stellar photometry. At the time of the Hipparcos Input Catalogue compilation only 49 per cent of these stars had photoelectric magnitudes and colours. The remaining stars had photographic or visual magnitudes. The cumulative distributions of standard errors on V magnitude for non-photoelectric, photoelectric and Hipparcos Hp magnitudes are shown in Figure 21.15. The transition from classical photoelectric photometry to the Hipparcos era represents a jump in accuracy similar to that from photographic to photoelectric, i.e. about one order of magnitude.

Magnitude Homogeneity

The intercomparison of stars over great circles of various orientations ensured the homogeneity of Hp magnitudes, free from systematic errors as a function, for example, of the star coordinates. The comparison with ground-based data reveals errors on classical photometry rather than on Hp magnitudes. For example the distribution of V residuals with respect to the declination, Figure 21.16, shows very small systematic errors as a function of declination, but an increase of quality for *UBV* data when obtained from southern sites, i.e. for $\delta < 10°$. With a mean error on $V\,(Hp)$ of 0.0032 mag, the external error on V_J appears to be about 0.026 mag.

The distribution of residuals over the whole sky is displayed in Figure 21.17 for V from *UBV* system. No large scale systematic errors, of the order of 1 per cent are noticeable although local departures are present. The comparison with Geneva magnitudes, Figure 21.18, shows little scatter locally over the sky but a modulation as a function of right ascension in the southern hemisphere with a peak to peak amplitude of 0.008 mag. The homogeneity of the Hipparcos photometric reference system is high enough to allow a complete re-evaluation of the star magnitudes as measured in the various photometric systems.

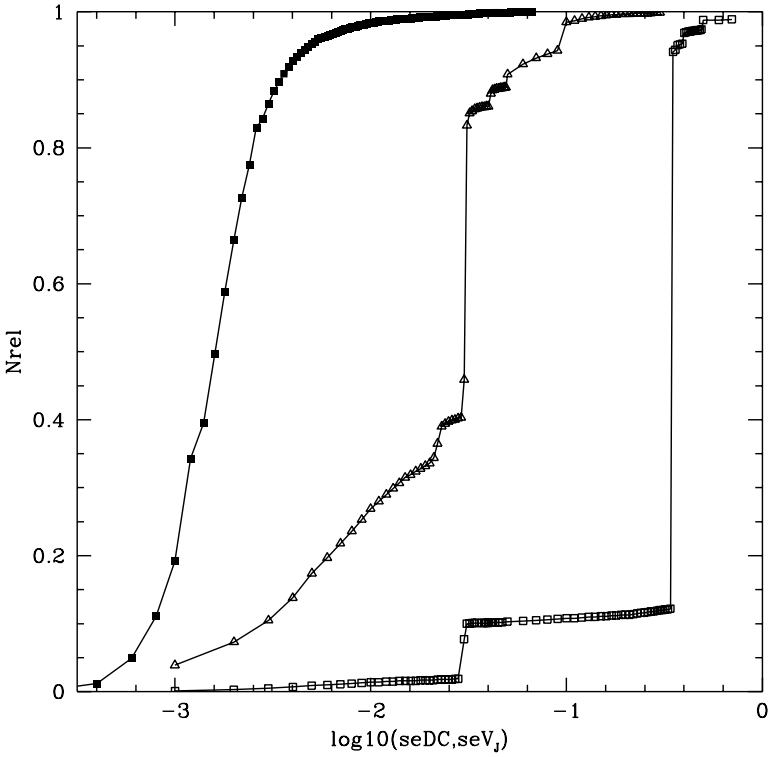

Figure 21.15. *The cumulative distribution of standard error on Hp magnitude (left curve), on photoelectric V magnitude (central curve) and on photographic or related visual magnitude (right-curve). The vertical jumps corresponds to assumed errors for single source data.*

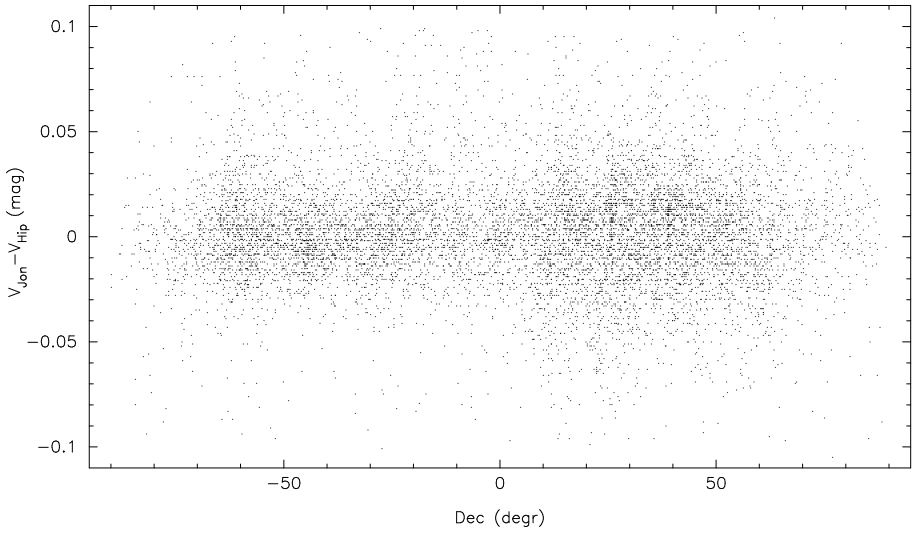

Figure 21.16. *The distribution of the residuals $V_J - V(Hp)$ for stars in common with UBV photometry and $V - I < 1.8$, as a function of declination.*

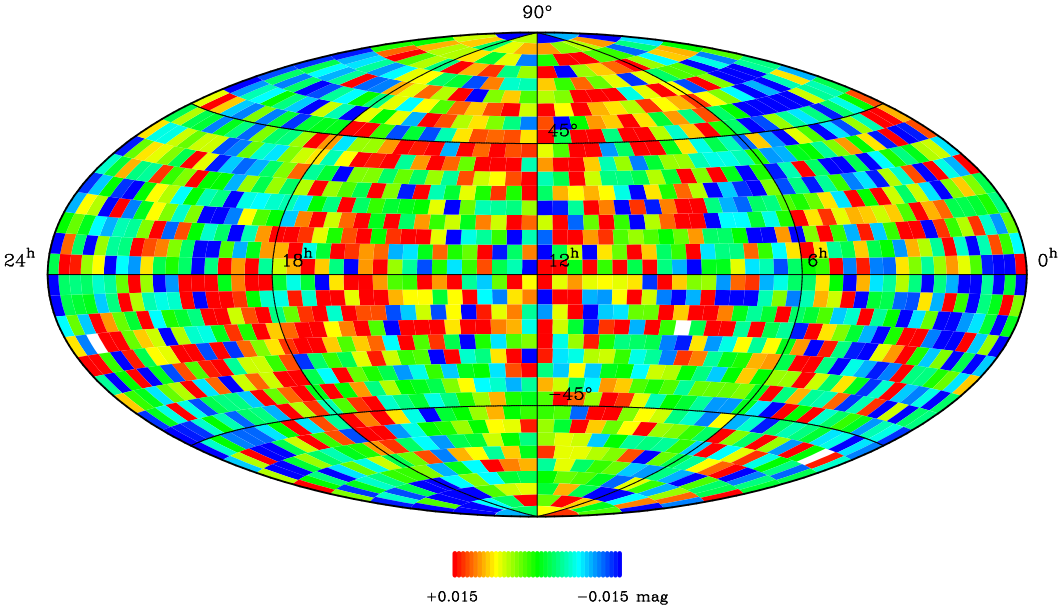

Figure 21.17. *The residuals $V_J - V(Hp)$ as a function of equatorial coordinates.*

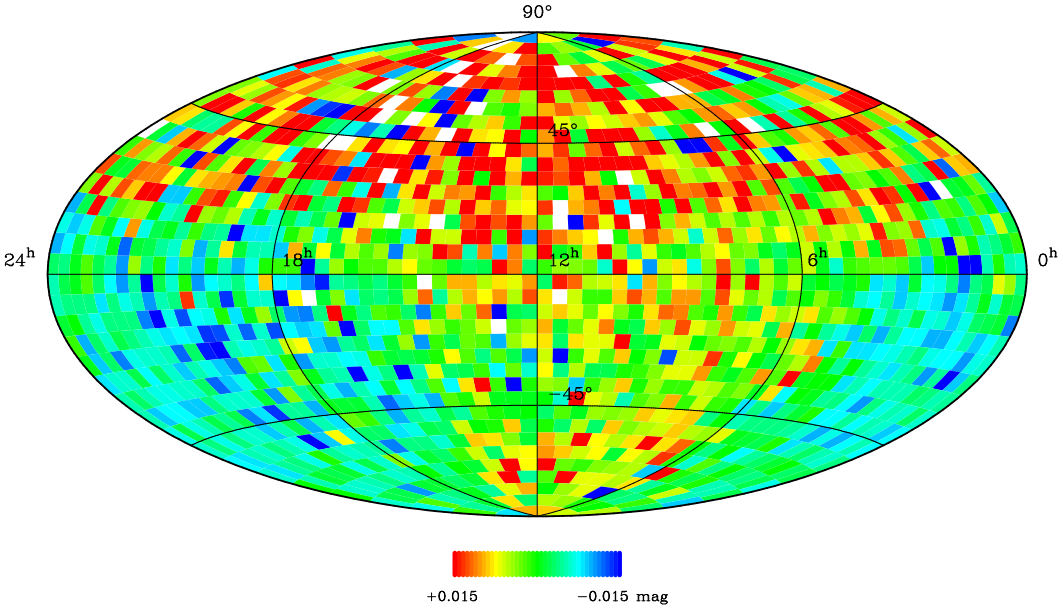

Figure 21.18. *The residuals $V_G - V(Hp)$ as a function of equatorial coordinates.*

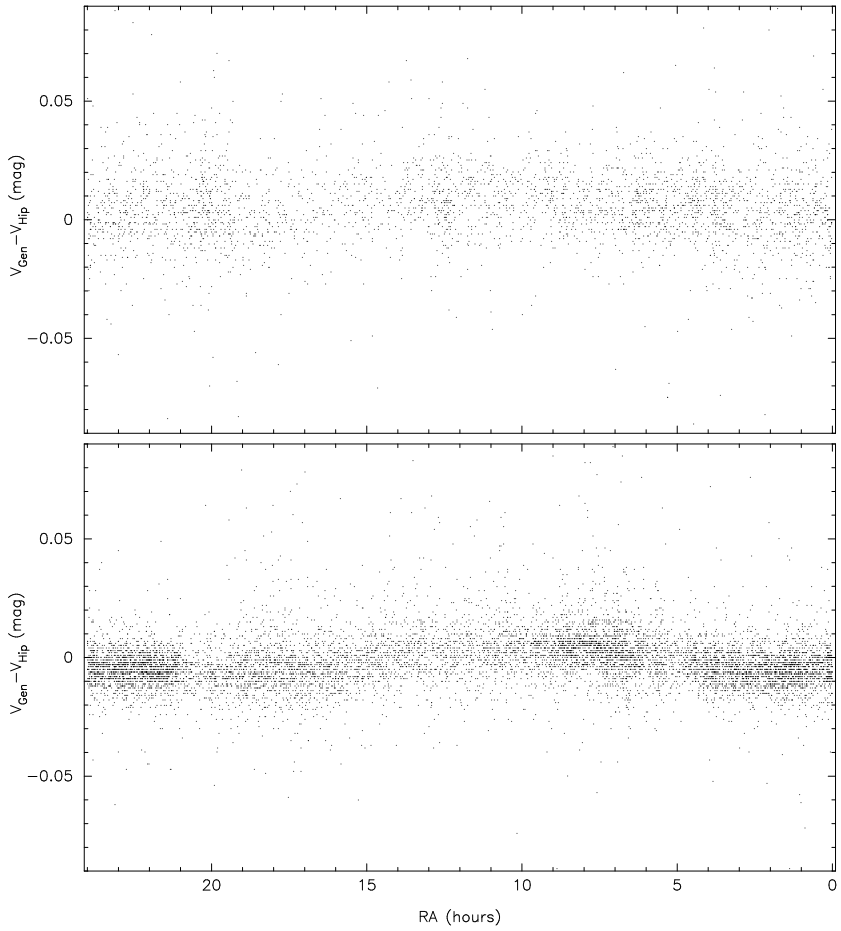

Figure 21.19. *The residuals V (Gen)–V (Hp) for stars with declination below 10° (bottom) and above 10° (top), as a function of right ascension.*

21.8. Conclusions

Unlike the situation that prevailed with the relative astrometry and photometry of the double stars, or to a lesser extent with the absolute astrometry of single stars, there was no real possibility of assessing the external quality of the photometric treatment from a comparison on a star-by-star basis, to ground-based data of comparable quality, for lack of material and the difficulty in making the transformation of the photometric system with the required accuracy. Therefore the various methods of validation attempted in this chapter had to rely mostly on the internal consistency rather than on an analysis of differences between Hipparcos photometry and independent external measurements. This was, however, possible on less quantitative aspects, such as the constancy of a limited set of bright stars or the comparison of the period of variables concluded from the Hipparcos data to their ground-based counterpart.

The comparisons do not reveal major shortcomings in the Hipparcos evaluation of the magnitudes and the estimate of the internal errors, except maybe for the very bright

stars ($Hp < 3$ mag) where the errors at the transit levels are probably a bit optimistic on the average. In this range as well, the Hp values may suffer systematic effects and should be used with care. The period determination appears of remarkable quality despite the relatively short time base for the long period variables, and the unfavourable observation window in many cases. Finally there are several pieces of information not evaluated here, but which constitute a major asset of the Hipparcos Photometric Catalogue: the alternate photometric scale ac, the indication for every transit of the complementary field of view and the identification of possible perturbing objects from the Guide Star Catalog. The value of this information should not be underrated in the astrophysical applications.

F. Mignard, M. Grenon, F. van Leeuwen